Supplementary Material for MM-Motion

Jiaqi Wu*
Beijing Sport University
Beijing, China
2025240795@bsu.edu.cn

Jianwei Li*†
Beijing Sport University
Beijing, China
jianwei@bsu.edu.cn

Ruiqi Ding
Beijing Sport University
Beijing, China
dingrq@bsu.edu.cn

Sixuan Wang
Beijing Sport University
Beijing, China
2023012548@bsu.edu.cn

Kehao Ran
Beijing Sport University
Beijing, China
rkh117@bsu.edu.cn

Rui Cao
Beijing Sport University
Beijing, China
caorui@bsu.edu.cn

ACM Reference Format:
Jiaqi Wu, Jianwei Li, Ruiqi Ding, Sixuan Wang, Kehao Ran, and Rui Cao. 2026. Supplementary Material for MM-Motion. In *Proceedings of ACM Multimedia 2026*. ACM, New York, NY, USA, 4 pages. https://doi.org/10.1145/nnnnnnn.nnnnnnn

Supplementary Materials

This supplementary material provides the detailed supporting contents for the main paper, including inter-annotator consistency analysis, complete action list, detailed scoring criteria for motion evaluation, and the description of model training.

A Detailed Action List of MM-Motion

Table 1 lists all 16 standardized actions and their functional categories.The collected movements were evaluated for injury risk from multiple dimensions, covering four major categories: unilateral support stability, dynamic directional control, static mobility and basic control, and landing buffering capacity. Hurdle stepping is a movement with extremely high demands on single-leg support and dynamic stability. Gribble et al.[3] noted that impaired single-leg balance is one of the most consistent clinical manifestations in patients with chronic ankle instability. Forward lunging actively challenges the positional stability of the talus in the ankle mortise and exposes deficits in the flexibility and stability of the hip, knee and ankle under asymmetric postures. Single-leg hopping directly assesses the ability of the periankle muscle-ligament system to absorb energy, maintain stability and respond rapidly under high-intensity, high-impact loading[1]. Macrum et al.[5] reported that improving ankle dorsiflexion mobility via Achilles tendon stretching significantly reduced foot eversion angles in subjects during squatting. Depth jumping accurately simulates the most common sprain scenario in sports and directly tests the capacity of the ankle and surrounding tissues to absorb high-impact energy[2].

*Both authors contributed equally to this research.
†Corresponding author.

Permission to make digital or hard copies of all or part of this work for personal or classroom use is granted without fee provided that copies are not made or distributed for profit or commercial advantage and that copies bear this notice and the full citation on the first page. Copyrights for components of this work owned by others than ACM must be honored. Abstracting with credit is permitted. To copy otherwise, or republish, to post on servers or to redistribute to lists, requires prior specific permission and/or a fee. Request permissions from permissions@acm.org.
ACM Multimedia 2026, Rio de Janeiro, Brazil
© 2026 ACM.
ACM ISBN 978-x-xxxx-xxxx-x/YYYY/MM
https://doi.org/10.1145/nnnnnnn.nnnnnnn

Table 1: Detailed Action List and Category, U.S.S.=Unilateral Support Stability, D.D.C.=Dynamic Direction Control, S.R.M.C.=Static Range of Motion and Control, L.B.C.=Landing Buffer Capacity.

ID	Action Name	Category
1	Hurdle Step - Right	U.S.S.
2	Hurdle Step - Left	U.S.S.
3	Straight Lunge - Right	U.S.S.
4	Straight Lunge - Left	U.S.S.
5	Single-Leg Hop - Right	D.D.C.
6	Single-Leg Hop - Left	D.D.C.
7	Single-Leg Squat - Right	S.R.M.C.
8	Single-Leg Squat - Left	S.R.M.C.
9	Squat	S.R.M.C.
10	Prone Calf Flexion and Elevation - Right	S.R.M.C.
11	Prone Calf Flexion and Elevation - Left	S.R.M.C.
12	Plantar Flexion and Dorsiflexion - Right	S.R.M.C.
13	Ankle Joint Rotation - Right	S.R.M.C.
14	Plantar Flexion and Dorsiflexion - Left	S.R.M.C.
15	Ankle Joint Rotation - Left	S.R.M.C.
16	Depth Jump	L.B.C.

B Excerpts from the Expert Evaluation Scale

Table 2 presents the Hurdle Step section of the expert evaluation scale. Each action is evaluated across three weighted dimensions, with sub-scores assigned to individual joints and detailed scoring key points provided.

C Expert Scoring Results and Analysis

C.1 Correlation between Expert Scores and CAIT Results

As shown in Figure 1, comparison between the final expert scoring labels and the Cumberland[4] Ankle Instability Tool(CAIT) results is illustrated in the figure. A total of 25 out of 31 subjects show identical risk levels in both assessment systems.

C.2 Consistency of Scoring Scales

This section analyzes the consistency of the overall score level and score dispersion among the three annotators, excluding systematic

Table 2: Scoring Rubric for Hurdle Step-Right, D.=Dimension, W.=Weight, S.=Score.

D.	W.	Joint	W.	Scoring Key Points	S.
Completion	4	Hip	1	Pelvis stable, no tilting	0-1
		Knee	3	Knee aligned with toes	0-3
		Ankle	5	Ankle stable	0-5
		Trunk	3	No swaying/lateral tilting	0-3
Accuracy	3	Hip	2	No rotation/lateral shift	0-2
		Knee	2	No valgus/varus	0-2
		Ankle	5	No inversion/eversion	0-5
		Trunk	3	No compensatory rotation	0-3
Fluency	3	Overall	4	No sudden swaying	0-4

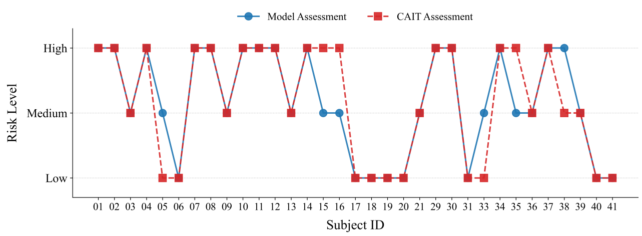

Figure 1: Consistency analysis between expert scoring labels and CAIT results, horizontal axis: Subject ID; vertical axis: Risk level.

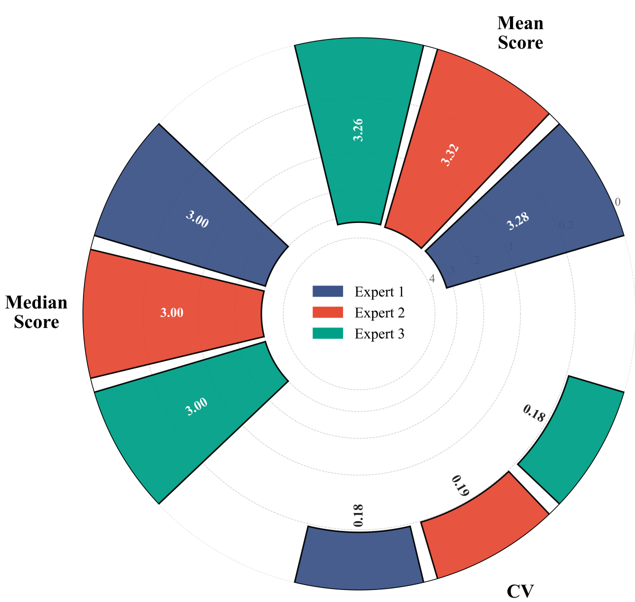

Figure 2: Comparison of mean scores, median scores, and coefficient of variation (CV) among three expert annotators, verifying the consistency of the scoring scale.

biases such as consistently high or low scoring by a single annotator. The consistency analysis chart is presented in the Figure 2.

The results verify the high consistency of the overall scoring scales across the three annotators, with no systematic bias of excessive leniency or strictness. For example, the average score of Annotator 2 is merely 0.07 points higher than that of Annotator 3, demonstrating highly comparable score dispersion.

C.3 Similarity of Action Score Distribution

To validate the consistency of annotators' judgments on action difficulty and quality, we analyze the relative ranking trends of the 16 actions across three scoring groups. The average scores of the 16 actions assigned by each annotator are ranked independently, with the lowest score labeled as 1 and the highest as 16. The spearman rank correlation coefficient (ρ)[6] is then calculated using the following standard formula:

$$\rho = 1 - \frac{6\sum_{i=1}^{n} d_i^2}{n(n^2-1)} \tag{1}$$

where:

- ρ: spearman rank correlation coefficient, ranging from $[-1, 1]$. A value closer to 1 indicates stronger ranking consistency;
- n: total number of actions ($n = 16$ in this study);
- d_i: rank difference of the i-th action between two annotators.

The inter-annotator consistency results are excellent:

- Annotator 1 and Annotator 2: $\rho = 0.83$ ($P < 0.001$), showing high consistency in scoring rank judgments;
- Annotator 1 and Annotator 3: $\rho = 0.81$ ($P < 0.001$), indicating excellent consistency;
- Annotator 2 and Annotator 3: $\rho = 0.79$ ($P < 0.001$), indicating excellent consistency.

D Experimental Software Interface Description

As shown in Figure 3, Figure 3(a) shows the interface during IMU data acquisition, which is used to monitor the wearing and connection status of IMU sensors, as well as the pre-acquisition calibration. Figure 3(b) presents the plantar pressure insole with 96 pressure sensors, which can effectively capture plantar biomechanical information during movement. Figure 3(c) displays the Kinect interface, including color image, depth image and thermal image streams.

E Model Training Description

We conducted two core experimental tasks: action recognition and injury risk evaluation, with the training curves of all models presented to verify their convergence performance and generalization ability.

E.1 Action Recognition Task

As shown in Figure 4 and Figure 5, in the action recognition task, we constructed unimodal action recognition models (including ST-GCN, LSTM, and other baseline architectures) based on three distinct modalities of motion data: IMU data, dual visual skeleton data, and plantar pressure insole data. The initial performance of these unimodal models was relatively poor. Further analysis of the model outputs revealed that movements with minimal upper-body

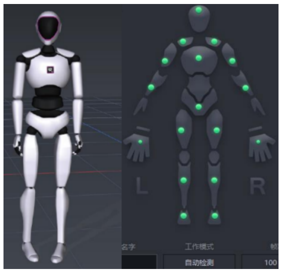

(a) Interface for collecting IMU data

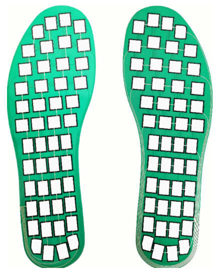

(b) Interface for collecting plantar pressure data

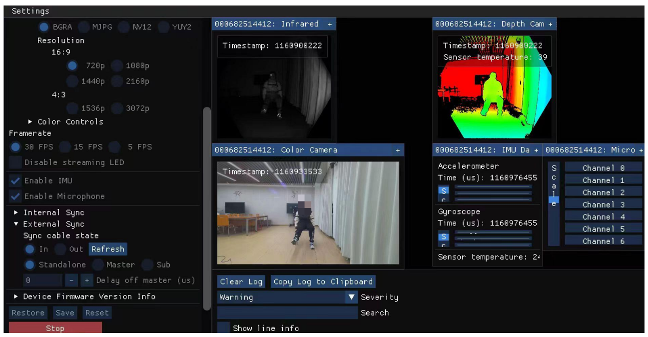

(c) Interface for collecting vision data

Figure 3: Software interfaces for data acquisition. (a) shows virtual character during IMU data collection; (b) shows 96 sensors on the plantar pressure platform; (c) shows three types of visual data interfaces.

motion (e.g., lower-limb focused actions related to ankle injury risk) were particularly difficult to recognize and distinguish accurately. To address this limitation, we introduced a lightweight attention mechanism to prioritize feature extraction from lower-body joint keypoints, enhancing the model's sensitivity to critical motion patterns. Additionally, for actions with negligible variations in upper-body joint data throughout the movement cycle, we directly zeroed out the upper-body feature streams to eliminate redundant noise interference, further improving the model's discriminative ability.

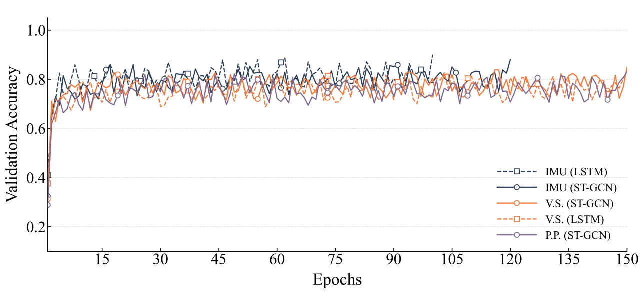

Figure 4: Validation accuracy curves of action recognition models during training. V.S.=Vision Skeleton, P.P.=Plantar Pressure.

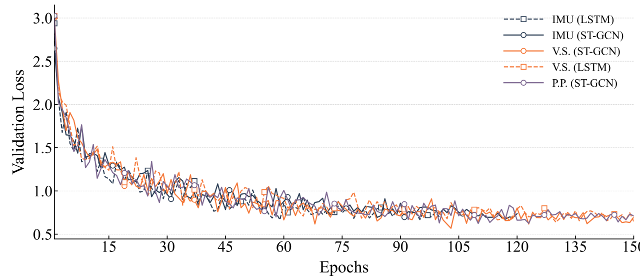

Figure 5: Validation loss curves of action recognition models during training.

E.2 Injury Risk Evaluation Task

As shown in Figure 6 and Figure 7, in the three-class injury risk evaluation task, we assessed the low, medium, and high injury risk levels of subjects. We built unimodal models based on four modalities of data, and finally fused them into a multimodal model. As shown in the figures, the proposed fused model achieves significantly improved performance compared with all unimodal baseline models.

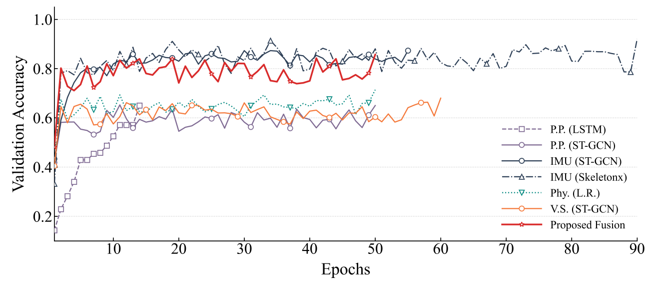

Figure 6: Validation accuracy curves of injury risk evaluation models during training.

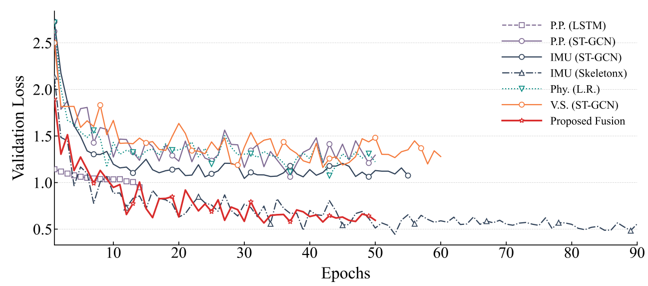

Figure 7: Validation loss curves of injury risk evaluation models during training.

F Acknowledgement

This work was supported by the Beijing Natural Science Foundation (No.4262068) and the Innovation Project of Sports Medicine Science and Technology of General Administration of Sport of China

(General Project No.2 of 2025). We sincerely thank Qian Kang and Chen Ziyao for their assistance during the data collection process.

References

[1] Rita S Chorba, David J Chorba, Lucinda E Bouillon, Corey A Overmyer, and James A Landis. 2010. Use of a Functional Movement Screening Tool to Determine Injury Risk in Female Collegiate Athletes. *North American Journal of Sports Physical Therapy : NAJSPT* 5, 2 (06 2010), 47–54.

[2] Siu Ngor Fu and Christina Wan Ying Hui-Chan. 2007. Are there any relationships among ankle proprioception acuity, pre-landing ankle muscle responses, and landing impact in man? *Neuroscience Letters* 417, 2 (2007), 123–127. doi:10.1016/j.neulet.2007.01.068

[3] Phillip A Gribble, Chris M Bleakley, Brian M Caulfield, Carrie L Docherty, François Fourchet, Daniel Tik-Pui Fong, Jay Hertel, Claire E Hiller, Thomas W Kaminski, Patrick O McKeon, Kathryn M Refshauge, Evert A Verhagen, Bill T Vicenzino, Erik A Wikstrom, and Eamonn Delahunt. 2016. Evidence review for the 2016 International Ankle Consortium consensus statement on the prevalence, impact and long-term consequences of lateral ankle sprains. *British Journal of Sports Medicine* 50, 24 (June 2016), 1496–1505. doi:10.1136/bjsports-2016-096189

[4] Claire E. Hiller, Kathryn M. Refshauge, Anita C. Bundy, Rob D. Herbert, and Sharon L. Kilbreath. 2006. The Cumberland Ankle Instability Tool: A Report of Validity and Reliability Testing. *Archives of Physical Medicine and Rehabilitation* 87, 9 (2006), 1235–1241. doi:10.1016/j.apmr.2006.05.022

[5] Robert W Moran, Anthony G Schneiders, Jesse Mason, and S John Sullivan. 2017. Do Functional Movement Screen (FMS) composite scores predict subsequent injury? A systematic review with meta-analysis. *British Journal of Sports Medicine* 51, 23 (2017), 1661–1669. doi:10.1136/bjsports-2016-096938 arXiv:https://bjsm.bmj.com/content/51/23/1661.full.pdf

[6] Philip Sedgwick. 2014. Spearman's rank correlation coefficient. *Bmj* 349 (2014).